Applied Geography 165 (2024) 103239

Contents lists available at ScienceDirect

Applied Geography

journal homepage: www.elsevier.com/locate/apgeog

High-resolution modelling of island exposure to natural hazards tested with real disasters

Nicolás Ferrer [a,*], Gustavo Herrera [b]

[a] Department of Geography, University of Las Palmas de Gran Canaria (IOCAG-ULPGC), Spain
[b] Cartográfica de Canaria S.A., Canary Islands Government (GRAFCAN), Spain

ARTICLE INFO

Handling Editor: J Peng

Keywords:
Natural risks
Human exposure
Dasymetric downscaling
Oceanic islands
Canary islands

ABSTRACT

Oceanic islands are multi-risk territories but statistical aggregation of socio-economic exposure data is often a constraint for high-resolution risk modelling and hazard prevention. This work presents a downscaling procedure to obtain a complete high-resolution cartographic base on the distribution of main socio-economic variables in the Canary Islands (Spain). For this purpose, a new dasymetric procedure has been developed based on the combination of cadastral censuses, detailed planimetries and LiDAR altimetry data. The methodology allowed for the construction of an exposure cartographic base (ECB) that comprises population, capital stock, productivity and heritage (cultural and natural) layers, covering the entire archipelago at 2.5 m resolution. The ECB results was tested for accuracy and found to be 90% accurate within a positional range of 50 m. The ECB was then compared with real damages in three recent natural disasters: a volcanic eruption on La Palma in 2021, a wildfire in Gran Canaria in 2019 and a coastal flooding in Tenerife in 2018. The comparison between modelled exposure and actual damage revealed the consistency of the cartographic base for full-damage events and the need to incorporate the vulnerability factor to obtain a more accurate estimate for partial damage events.

1. Introduction

Oceanic islands tend to be risk-concentrated territories due to their natural hazardousness and human population density (Audru et al., 2010; López-Saavedra & Martí, 2023; Richmond et al., 2001). Although some remote islands do not have stable human settlements today (e.g., Trindade, Crozet Islands), many others are very densely populated exposed to natural hazards (e.g., Canary Islands, Hawaii, Mauritius, Bermuda, Comoros) (Fig. 1a). In addition, their small size and fragmentation limit the availability of resources and reduce the adaptability of populations to a temporary decline in productive systems, while their isolation and remoteness from continental territory can delay responses to natural disasters and make external assistance difficult (López-Saavedra and Martí, 2023; Pelling & Uitto, 2001).

Volcanism is an inherent hazard due to the volcanic origin of oceanic islands. Young islands at the active ends of insular chains rank among the most eruptive hotspots on the planet. Volcanoes such as Kilauea (Hawaii), Cumbre Vieja (Canary Islands) or Pico do Fogo (Cape Verde) are among the most active in the world. The eruption of Karthala led to the evacuation of thousands of people from Grande Comore in 2005 (Bachèlery et al., 2015), while the Tajogaite eruption on the island of La Palma generated one of the most recent volcanic emergencies (Carracedo et al., 2022). Mauna Loa is the largest volcanic edifice on the planet and threatens much of the population of the Big Island of Hawaii (Genzano et al., 2023; Wright et al., 1992). In addition, intense eruptive activity in the growth phases of oceanic islands produces gravitational instability and flank collapse (e.g., Masson et al., 2008). Although not directly observed, mega-landslides are intrinsic to island development and can be highly catastrophic, involving huge land masses. The multiple records of the generation of extraordinarily large tsunamis caused by oceanic island flank collapses indicate that the threat is twofold. The landslide on Fogo Island (Cape Verde) approximately 70,000 years ago pushed blocks weighing hundreds of tonnes to altitudes of more than 200 m on the neighbouring island of Santiago (Ramalho et al., 2015). Ward and Day (2001) warned of the potential slide of Cumbre Vieja (La Palma) and the large tsunami that could be generated in the Atlantic. However, tsunamis caused by earthquakes in are more frequent than those triggered by landslides, and their recurrent impact is favoured by the exposure of oceanic islands to waves in large maritime regions. For example, the Mascarene Islands are highly exposed to tsunamis originating from the Java-Sumatra subduction zone (Allgeyer et al., 2017). The last major Indian tsunami in 2004 impacted and caused material

* Corresponding author.
E-mail address: nicolas.fvg@ulpgc.es (N. Ferrer).

https://doi.org/10.1016/j.apgeog.2024.103239
Received 11 September 2023; Received in revised form 16 February 2024; Accepted 20 February 2024
Available online 24 February 2024

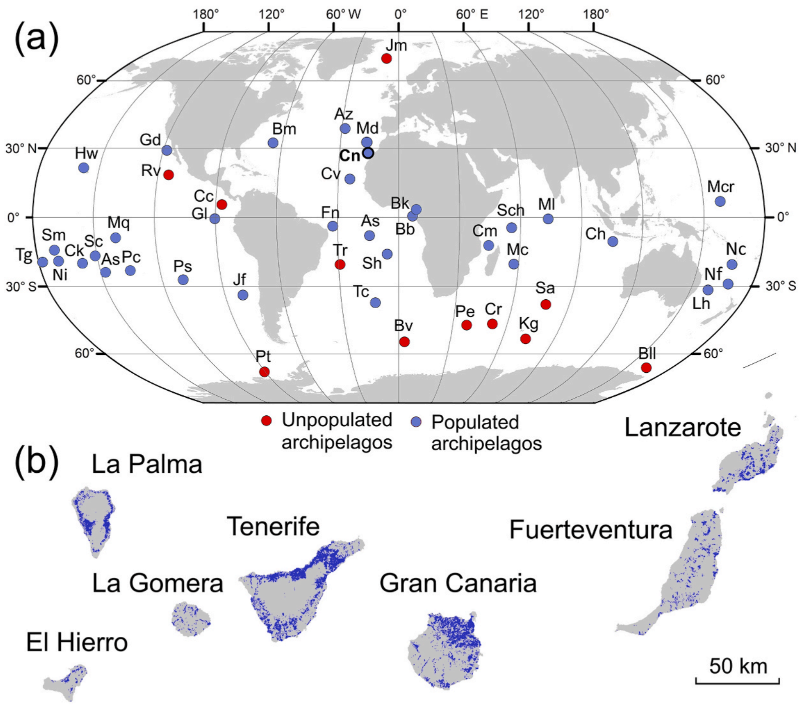

Fig. 1. (a) World map of some of the main oceanic archipelagos with indication of the existence of human settlements. Archipelagos with geological parallels to the Canary Islands, the case study, are represented, so subduction-edge volcanic islands are not shown. As, Ascension; As, Australs; Az, Azores; Bb, Bight of Bonny; Bll, Balleny; Bv, Bouvet; Cc, Cocos; Ch, Christmas; Ck, Cook; Cm, Comoros; Cn, Canary; Cr, Crozet; Cv, Cape Verde; Fn, Fernando de Noronha; Gd, Guadalupe; Gl, Galapagos; Hw, Hawaii; Jf, Juan Fernandez; Jm, Jan Mayen; Kg, Kerguelen; Lh, Lord Howe; Mc, Mascarene; Mcr, Micronesia; Md, Madeira; Mq, Marquesas; Nc, New Caledonia; Nf, Norfolk; Pc, Pitcairn-Tuamotu; Pe, Prince Edward; Ps, Easter Island; Pt, Peter; Rv, Revillagigedo; Sa, Saint Paul and Amsterdam; Sc, Society; Sh, Saint Helena; Sm, Samoa-Gilbert; Tc, Tristan da Cunha; Tg, Tonga; Tr, Trindade and Martin Vaz.(b) Map of the Canary Islands and (in blue) current distribution of human settlements (population data from ISTAC, Canary Islands Government, 2018).

damage on La Réunion, where the population is heavily concentrated along the coastline; and in September 2009 Samoa and Tonga were hit by a tsunami that killed 189 people (Okal et al., 2010). Earthquakes associated with magmatic activity in intra-plate regions are usually of low intensity, but archipelagos such as the Azores and Samoa have a long history of catastrophic earthquakes associated with transform fault activity or proximity to subduction zones. In 1980, a Mw 7 earthquake devastated the islands of Terceira, São Jorge and Graciosa, killing more than 60 people and destroying thousands of houses (Carvalho, 1980).

Extreme weather events are also common on many oceanic islands. Some tropical archipelagos are located in areas which potentially devastating hurricanes or cyclones commonly pass through. For example, Bermuda receives an average of six hurricanes every year. In 2010, thousands of people had to be evacuated from Tahiti and Bora Bora due to the arrival of Cyclone Oli, and Hurricane Lane caused catastrophic flooding in 2018 in Hawaii (Callaghan, 2019). In late 2012, Samoa was severely affected by Cyclone Evan, which killed 5 people and displaced thousands (Meldau, 2013). Other extratropical archipelagos also experience potentially destructive extreme rainfall events. The subtropical archipelagos of Madeira and the Canary Islands are prone to severe flooding events from strong Atlantic squall discharges over steeply sloping short watersheds. Torrential rains on the island of Madeira in February 2010 left 45 people dead and destroyed multiple infrastructures due to landslides (Fragoso et al., 2012). Seasonal aridity is also a problem in archipelagos such as the Canary Islands, Madeira or the Galapagos, causing severe droughts and the development of large-scale wildfires, greatly favoured by the rugged terrain and constant winds. In Madeira, 6000 ha burned in August 2016, resulting in the deaths of 3 people and nearly 60 million euros worth of damage (Couto et al., 2021). Most recently, in Maui (Hawaii), the fires of August 2023 were one of the worst natural disasters in US history, with more than 100 deaths and billions of dollars in material damage (Arango et al., 2023).

In the multi-hazard scenario of oceanic islands, human exposure is a critical component because the natural catastrophes occur in the encounter of destructive physical phenomena with populations and material assets (e.g., Petak and Atkisson, 1982; Tobin, 1997, pp. 8–10; Iglesias et al., 2021). In this sense, Iglesias et al. (2021) noted that the increase in losses associated with disasters is often due to increased human exposure in hazardous areas, while other authors (Formetta & Feyen, 2019; Jongman et al., 2015; Paprotny et al., 2018) reported how improved hazard prediction, protection and warning systems have produced an overall decrease in damages per exposed unit in recent decades.

Given the importance of the exposure factor, spatial planning of land uses has become a basic form of risk prevention by locating human activity away from hazardous areas (Burby, 1998, pp. 9–10; Campbell, 2019, p. 46). Spatially explicit information on the geographical distribution of population, property and economic assets is therefore essential for assessing risks, designing preventive planning and improving response systems (Ehrlich et al., 2018; Iglesias et al., 2021; Lerner-Lam, 2007). However, this information is either non-existent or insufficiently detailed in many countries and regions (Ehrlich et al., 2018), a fact that is especially noticeable in many developing island territories (Pelling et al., 2001). Existing socio-economic data usually come from official agencies, aggregated into administrative units that do not allow for accurate exposure observation and introduce significant errors in risk estimation (Chen et al., 2004). The importance of improving knowledge on socio-economic exposure worldwide has led to the development in recent decades of numerous projects to generate exposure mapping databases at different scales, including global (e.g., Ehrlich et al., 2018; Geiger, 2018; Jongman et al., 2015; Kummu et al., 2018; Lerner-Lam, 2007; Pesaresi et al., 2017), continental (e.g., HVRI, 2015; FEMA, 2002; Paprotny et al., 2018), regional (e.g., Fuchs et al., 2017) and local (e.g., Keiler, 2004; Keiler et al., 2006; Lirer et al., 2010). In islands of oceanic

Table 1
Primary sources of socio-economic variables used to construct the exposure cartographic base.

Data	Source/Agency	Information	Scale/Resolution	Year
Population map	ISTAC (Canary Islands Government)	Distribution of resident population	Grid 250 × 250 m	2018
Tourist Accommodation Survey	ISTAC (Canary Islands Government)	Tourist population distribution	Tourist centres	2010–2019
Cadastral value of assets and infrastructure	General Cadastre Directorate (Government of Spain)	Distribution of capital stock (€)	Municipal	
Capital stock and services	BBVA Foundation	Distribution of capital stock (€)	Provincial	2019
Gross Domestic Product (GDP) by sector	INE (Government of Spain)	Added value of production (€/year)	Insular	2010–2018
Value of agricultural production	ISTAC (Canary Islands Government)	Overall value of production (€/year)	Provincial	2010–2011
Value of energy production	INE (Government of Spain)	Overall value of production (€/year)	Regional	2010–2018
Tourism income	ISTAC (Canary Islands Government)	Income (€/year)	Tourist municipalities	2019

regions where data are particularly scarce, some recent efforts to determine socioeconomic exposure to natural hazards should be highlighted, particularly in Pacific islands (Andrew et al., 2019; Thomas et al., 2023; Williams et al., 2021).

The aim of this work is to contribute to overcoming data constraints in the quantification of socioeconomic exposure to natural hazards in island contexts by providing a new dasymetric procedure (Eicher and Brewer, 2001; Mennis, 2009) for mapping socioeconomic variables at high resolution from existing low-resolution data. The proposed procedure is based on a new way of combining cadastral censuses, detailed planimetries and LiDAR altimetry data. The method is consistently applied to a range of socio-economic indicators (not just the population as in the vast majority of dasymetry-based studies) of the entire archipelagic territory of the Canary Islands. The ultimate goal is to provide an accurate and reliable basis for the assessment of natural hazards in this region, which is currently lacking. It is important to note that the Canary Islands form part of the European Union and therefore enjoy a more efficient administrative structure and have more datasets available compared to most other volcanic island territories in the world.

2. Study area

The Canary Islands are located in the northeast Atlantic, at about 28° north latitude and 15° west longitude (Fig. 1b). They form a chain of seven main islands (Lanzarote, Fuerteventura, Gran Canaria, Tenerife, La Gomera, La Palma and El Hierro), totalling 7447 km^2 and ~1500 km of coastline. Politically, they form one of Spain's seventeen Autonomous Communities and have the status of Outermost Region of the European Union. Since the beginning of the 20th century, socio-economic exposure in the Canary Islands has been steadily increasing, with a rising population which has accelerated in growth since 1960. It currently has a total of 2,176,412 inhabitants and a population density of 292.19 inhabitants/km^2 (INE, 2022). It is the largest, most densely populated and economically active archipelago in the natural region of Macaronesia, of which the Atlantic archipelagos of Cape Verde, Madeira (Portugal) and Azores (Portugal) also form part.

The predominant natural hazards in the Canary Islands are volcanism, river and coastal flooding, landslides and wildfires. The Canary Islands are the geological product of eruptive activity since the Tertiary Era in the transition zone of the oceanic and continental crust of Africa, making it one of the most volcanically active areas in the Atlantic. All the islands, except La Gomera and Gran Canaria, have experienced historical eruptions, including, for example, the major eruption of Timanfaya on Lanzarote and the numerous recent eruptions on La Palma (Carracedo et al., 2022; Hernández-Pacheco & Valls, 1982). In addition, the Canary Islands have a coastline of more than 1500 km which is subject to predominantly NNE winds combined with North Atlantic swells. Storm surges occur predominantly in the winter months and often reach significant wave heights of more than 5 m and peak periods of more than 15 s (Yanes, 2012, 2017). The risk of coastal flooding in the Canary Islands is exacerbated by the high levels of human concentration in coastal areas, driven mainly by the urban-tourism sector since the 1960s (Yanes, 2012, 2017). More than 80% of the population of the Canary Islands currently live less than 5 km from the coastline (ISTAC, 2018), where most of the infrastructures and production activities have also been developed. In turn, the archipelago has extensive forests in the midlands and summits of the central (Gran Canaria and Tenerife) and westernmost (La Gomera, El Hierro and La Palma) islands. Every year, especially during the dry summer months, fires of different magnitude occur, entailing serious socio-economic risks. The risk increases notably due to the type of settlement in these areas, which is highly dispersed and intertwined in urban-forest and agricultural mosaics. Once a wildfire starts, the complex orography and steep slopes of the islands favour its spread and hinder its extinguishing (DGSE, Canary Islands Government, 2014).

3. Methodology

3.1. Variables and sources

The exposure cartographic base (ECB) that has been developed includes spatially explicit information on population, economic assets and natural and cultural heritage elements. The initial data were collected from official statistics from public or private regional and national entities, which were free to access (Table 1).

The population was divided into resident and tourist. The resident population was obtained from the Demographic Statistical Grid of the Canary Islands (ISTAC, Canary Islands Government), which includes a population quantification on a 250 × 250 m resolution grid for the year 2018. The tourist population in the Canary Islands was taken from the Tourist Accommodation Survey (ISTAC, Canary Islands Government), which annually aggregates visitor data at the level of tourist nuclei. The Equivalent Tourist Population indicator was used, which provides the number of tourists staying on an average day of the year (i.e., the amount of tourist population at a given time, which is the most relevant indicator for the analysis of exposure to natural hazards).

Economic assets were divided into capital stock (eur) and productivity (eur $year^{-1}$). The updated capital stock of tangible assets and infrastructures was taken from the rural and urban cadastral values, aggregated at the municipality level by the General Cadastre Directorate (Government of Spain), and from capital stock and services statistical data, aggregated at the provincial level by the BBVA Foundation (2019). The productive value was taken from the statistical data, aggregated at island level, of the annual GDP of the primary, secondary and tertiary sectors obtained from the National Statistics Institute (INE, Government of Spain). Due to its economic and strategic relevance for the Canary Islands, from the primary sector we marginally obtained the annual value of agricultural production, aggregated at provincial level by the Canary Islands Statistics Institute (ISTAC, Canary Islands Government), from the secondary sector the annual value of energy production, aggregated at regional level by the INE (Government of Spain), and from the tertiary sector the annual tourism income, aggregated at the level of tourist municipality by ISTAC (Canary Islands Government).

Finally, heritage was divided into natural and cultural, and was incorporated into the ECB from the official planimetries. In total, 146 protected natural sites from the Canary Islands network (CTEE, Canary Islands Government), 222 protected natural sites from the European network (CTEE, Canary Islands Government), 278 geoheritage sites

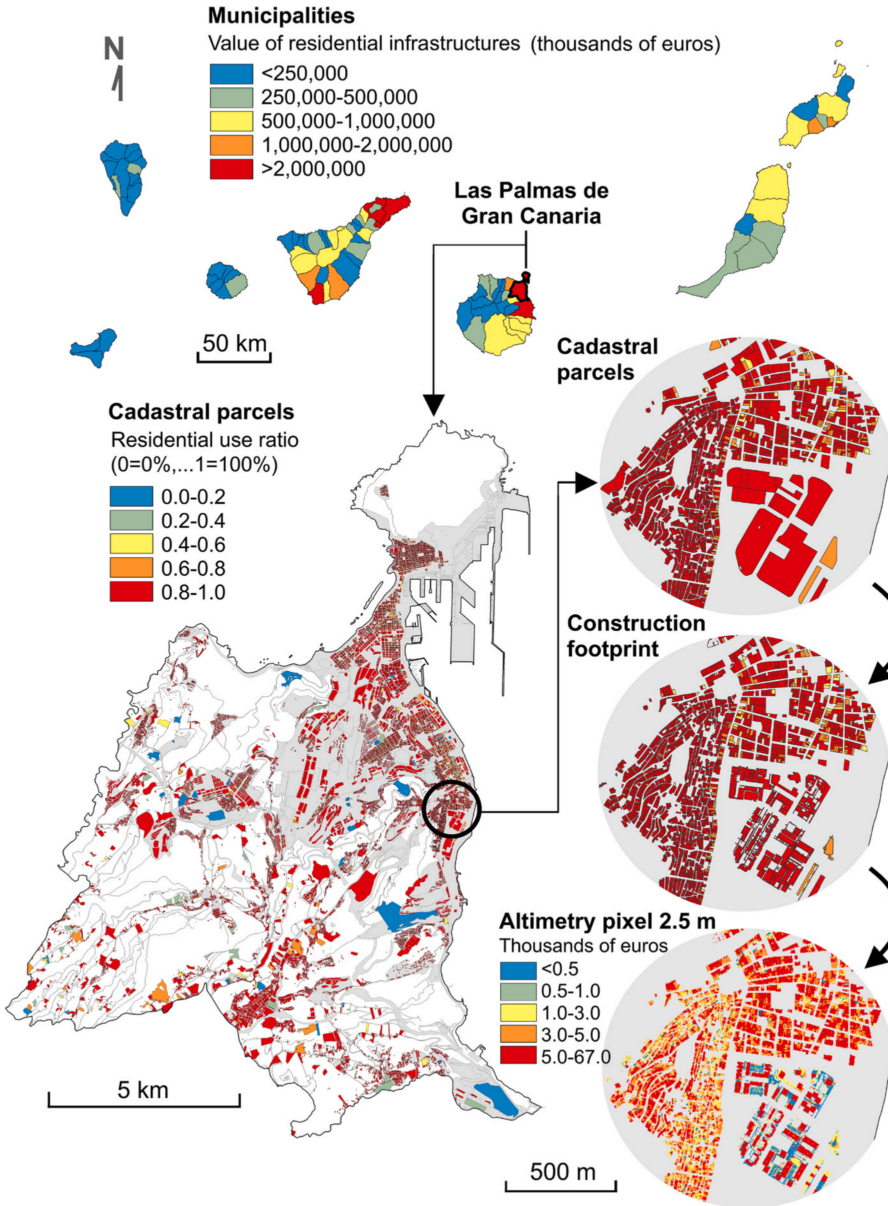

Fig. 2. General downscaling flow chart for the construction of the Exposure Cartographic Base (ECB) of the Canary Islands.

(IGME, Spanish Government) and 343 cultural heritage sites, regionally named after their initials in Spanish (BIC) (Canary Islands Government and insular councils), were incorporated into the ECB.

Regional censuses of facilities, infrastructure and economic activities were used to test the positional accuracy of the ECB results. The tests were carried out by calculating Euclidian distances of the ECB from the punctual records of the Tourist Accommodation Survey (ISTAC, Canary Islands Government), the Census of Industrial Land (General Directorate of Industry and Energy, Canary Islands Government), the Census of Educational Centres (Board of Education, Universities, Culture and Sports, Canary Islands Government) and the Street Map of the Canary Islands (GRAFCAN, Canary Islands Government).

3.2. Socioeconomic downscaling

The downscaling method used is dasymetric. Dasymetry is one of the most accurate interpolation technique for estimating the spatial distribution of people and goods in the absence of scaled data (Wu et al., 2005). It consists of refining the distribution of an aggregated geographical variable in statistical units by means of auxiliary spatial information (Chen et al., 2004; Eicher and Brewer, 2001; Mennis, 2009) and has been applied especially in the spatial disaggregation of population censuses (e.g. Chen et al., 2004; Eicher and Brewer, 2001; Gallego et al., 2011; Holt and Lu, 2011; Jega, 2015; Lwin and Murayama, 2011; Maantay et al., 2007; Mennis, 2003; Su et al., 2010).

The first dasymetric level consisted of reducing the indicators contained in the original statistical entities to the cadastral parcels (Fig. 2a). Following the CEDS of Maantay et al. (2007), we used census information from the cadastral base of Spain (General Cadastre Directorate, Government of Spain) to obtain the highest possible spatial and typological resolution. The cadastral cartography of Spain comprises planimetric and alphanumeric information of uses in both rural and urban parcels of the whole territory of the Canary Islands. It also includes information on the vast majority of buildings that could be considered precarious.More than 1,300,000 plots were processed to calculate the proportion of each land use inside the parcels, assigning values between 0 and 1 (0 = 0%, … 1 = 100%). For their part, the annual socio-economic indicators (Table 1) were averaged for the period

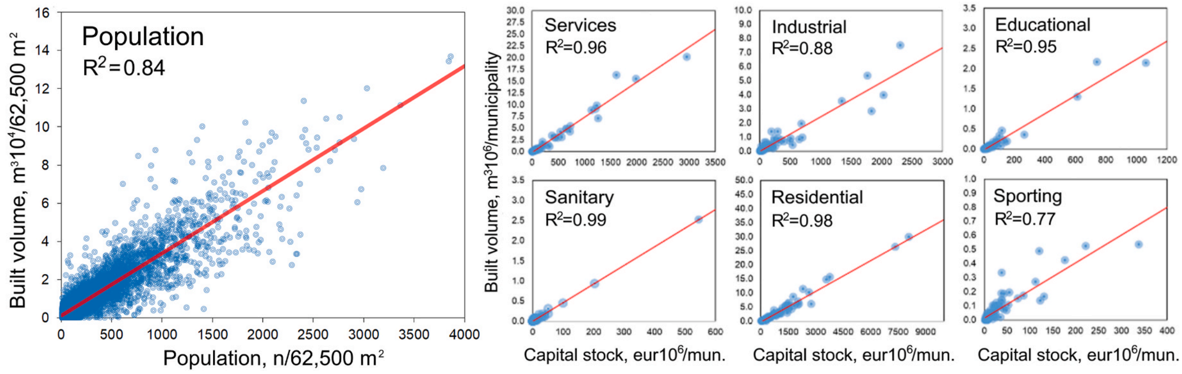

Fig. 3. Observed correlation between built volume and socio-economic variables. In the larger graph on the left, the relationship is shown between population and the volume of residential buildings in the demographic grid of 250 m squares. In the smaller graphs on the right, the relationship is shown between the cadastral value of infrastructures and their built volume in the 88 municipalities of the Canary Islands. The high correlations justify the use of LiDAR altimetry as a downscaling disaggregator variable for economic indicators in the Canary Islands.

2010–2019 and incorporated as an attribute to their respective geographic vector entities (e.g., cadastral value→municipalities; sectoral GDP→islands). They were subsequently reduced to cadastral parcels with coinciding use by means of geographical intersection operations in GISs (e.g., resident population→parcels of residential accommodation use; tourist population→parcels of tourist accommodation use; industrial GDP→parcels of industrial use).

The second dasymetric level involved reducing the indicators contained in the cadastral plots exclusively to the construction footprint (Fig. 2b). Particularly in rural and sparsely dense urban environments in the Canary Islands, parcels can be much larger than the built-up land they contain, and so this bounding is necessary to achieve a good level of spatial accuracy. In the opposite cases, especially in dense urban areas, the parcels are equal to or smaller than the built-up space, which they divide, and the spatial distribution of parcel uses remains unaltered after the intersection. For this operation, the official cartographic base of the Canary Islands (GRAFCAN, Canary Islands Government) was used, which contains updated information on infrastructures, constructions and basic structural elements of the territory at a scale of 1:1000/1:5000. From this cartographic base, the construction footprint was extracted, considering as such paved grounds, generic constructions (warehouses, walls, deposits, silos, stairways, swimming pools, transformers, canopies, etc.) and buildings. By means of spatial intersections in GISs, the socio-economic variables contained in the cadastral plots were reduced to the built-up part. In this operation, the land use values from 0 to 1 (0 = 0%, … 1 = 100%) were conserved.

The third dasymetric level entailed disaggregating the values contained in the construction footprint according to 2.5 × 2.5 m LiDAR pixel volumetry (Fig. 2c), assuming that they are distributed proportionally to the volumetric magnitude (Lwin and Murayama, 2011). For example, residential buildings house more population in proportion to their volume. Built volume was chosen because it is a geographically consistent variable and strongly correlated linearly with socio-economic indicators at the level of their respective aggregation entity in the Canary Islands (Fig. 3). It explains, for example, 84% of the spatial variations in population volume in the archipelago. Built volume was obtained from LiDAR-derived digital elevation models at 2.5 m resolution (GRAFCAN, Canary Islands Government, 2012–2020), using the construction footprint as a spatial constraint. From the product of the proportion of a use (α) and the height above ground of the construction (β), it was possible to estimate a three-dimensional space for that use (use space) in each pixel of 2.5 m resolution. In order to respect the pycnophylactic principle (Tobler, 1979), the final pixel value of a downscaled socio-economic indicator (V) was obtained by multiplying the original aggregate value of the indicator (ρ) by the ratio of the pixel's use space (αβ) to the total use space in the whole statistical aggregation entity (∑αβ) (Equation (1)).

Table 2
Correspondence of the ECB results with different censuses of activities and facilities in the Canary Islands. The percentages are with respect to the total number of points, and the metric values correspond to the distance to the elements of the same type in the ECB.

Control maps	Number of control points	Distance to the ECB (m)			
		50%	75%	90%	95%
Tourist accommodation[a]	1792	<50	<50	<150	<300
Industrial plants[b]	203	<50	<100	<200	<300
Educational centres[c]	1324	<50	<50	<100	<250
Commercial facilities[d]	656	<50	<50	<100	<150
Sports facilities[d]	1800	<50	<50	<250	<550
Health facilities[d]	350	<50	<50	<50	<200
Religious buildings[d]	1181	<50	<50	<50	<350
Emergency services[d]	401	<50	<450	<1000	>1000
All	7707	<50	<50	<100	<250

[a] Canary Islands Tourist Accommodation Survey (ISTAC, Canary Islands Government).
[b] Census of Industrial Land in the Canary Islands 2017 (General Directorate of Industry and Energy, Canary Islands Government).
[c] Pre-school, primary and secondary schools (Board of Education, Universities, Culture and Sports, Canary Islands Government).
[d] Street Map (GRAFCAN, Canary Islands Government).

$$V=\rho\left(\alpha\beta\Big/\sum\alpha\beta\right) \qquad \text{Eq. 1}$$

3.3. Exceptions completing the ECB

Exceptions to the general cadastral-volumetric procedure were made for agricultural economic values, road infrastructures and electricity production plants. The thematic agricultural cartography used was the Crop Map of the Canary Islands (Ministry of Agriculture, Livestock, Fishing and Food, Canary Islands Government), updated between 2017 and 2021 by means of exhaustive field and photo-interpretative studies at a scale of 1:2000. In these cases, a weighted distribution method was chosen. In the agricultural sector, the productive value was uniformly disaggregated by cultivated area, applying a 30% higher productivity to greenhouse-based areas. For road infrastructures, a uniform distribution of the value was made by applying a weighting in geometric progression according to the hierarchy of the road and the presence of tunnels or bridges (roads = 1–2, streets = 4–8, conventional roads = 16–32, motorways and dual carriageways = 64–128). For electricity production plants, a limited distribution was applied to the approximate global weight of electricity production in the Canary Islands by source type

Table 3
Summary of the ECB exposure of population, capital stock, productivity and heritage during the Tajogaite volcano eruption (La Palma, Canary Islands, 2021), the Artenara and Valleseco wildfire (Gran Canaria, Canary Islands, 2019) and the Garachico coastal flooding (Tenerife, Canary Islands, 2018).

		La Palma eruption 2021		Gran Canaria wildfire 2019		Tenerife flooding 2018	
Event magnitude (hm^2)		1201.2		10,334.2		9.1	
Exposure		ECB	ES	ECB	ES	ECB	ES
Population (n)	Resident	2810		3005		34	
	Tourist	44		15		82	
	Total	2854	3200	3020	11,500	116	39
Capital stock (€ 10^3)	Residential	83,068		28,173		3194	
	Health	69		15		9	
	Education	688		1036		286	
	Sports	1358		8		1367	
	Historic/relig.	139		190		93	
	Transport	8081		38,623		119	
	Non-built urb.	2398		1998		88	
	Agricultural	1,008,606		697,496		–	
	Industrial	10,860		3748		70	
	Services	4605		1280		1256	
	Other	380		16		110	
	Total	1,120,252		772,581		6594	
Production (€/year 10^3)	Primary	4484		3031		–	
	Industrial	9576		5009		52	
	Tertiary	13,174		4205		5430	
	Total	27,234		12,244		5482	
Total economic (€ 10^3)		1,147,486	1,051,000	784,826	18,000	12,076	807
Heritage (n)	Cultural	2		10		3	
	Natural	4		17		2	
	Total	5		27		5	
Heritage (hm^2)	Cultural	0.6		524.5		6.8	
	Natural	88.1		9834.6		7.4	
	Total	88.7		9834.6		7.4	

[a]The total surface area of the heritage elements is less than or equal to the sum due to possible overlap between them. ECB, value of the exposure cartographic base; ES, mean value of the external sources.

(thermal = 90%, wind = 6%, solar = 3%; hydroelectric = 1%).

4. Results

4.1. Positional cross-check of the ECB with equipment censuses

Part of the ECB results were compared with regional censuses, which constitute point maps used as control data. From the comparison of distances between the ECB and the point censuses, a generally high thematic and positional accuracy was found (Table 2). In the 8 thematic areas tested (tourist accommodation, industrial plants, educational centres, commercial facilities, sports facilities, health facilities, religious buildings and emergency services), at least 50% of the census points were less than 50 m away from their corresponding elements in the ECB. As we increased the sample of census points, the confidence distance remained within acceptable ranges: 90% of the census points were at distances of less than 50 m from their corresponding areas in the ECB. Of the educational centres, commercial facilities and health facilities surveyed, 95% were within 250 m of their ECB counterparts. In the case of tourist accommodation, industrial plants and religious buildings, the distance range increased to as much as 350 m from the ECB for 95% of the surveyed points, and in the case of sports facilities to 550 m. The lowest accuracy was found for emergency services, although 75% were located within 450 m and 90% within 1 km. Overall, 95% of the points surveyed were at distances of under 250 m from their ECB counterparts, and hence it can be concluded that a good general level of fit of the ECB to the real scale was obtained.

4.2. Exposure and damages in the 2021 La Palma volcanic eruption

The 2021 Tajogaite eruption took place on the Cumbre Vieja volcanic ridge in a densely populated area of the island of La Palma known as Los Llanos de Aridane (Fig. 5). It started at the end of September 2021 and lasted for 3 months, during which time more than 150 million cubic metres of lava were emitted (Cívico et al., 2022) covering an area of 12.25 km^2. Successive lava flows progressed downhill for more than 5 km before reaching the sea (Ferrer, Marrero-Rodríguez, Sanromualdo-Collado, Vegas, & García-Romero, 2023). Numerous houses, infrastructures and agricultural areas were destroyed, but there was no loss of life due to the slow movement of the lava flows and the rapid action of the civil protection services (Troll et al., 2023).

Due to the characteristics of the area, the greatest impact was on the population and economic resources (Table 3). Of the affected population, 98% were residents according to the ECB. With respect to the area impacted by the eruption, 2810 residents lost their homes according to the ECB, although the number of people evacuated during the emergency exceeded 7000 (Decree-Law 1/2022 of 20 January). The ECB-based number is close to the figure of 2329–2748 affected people reported in the Territorial Framework for Post-Eruption Recovery (García-Rodríguez, 2023; Vargas, 2023). While 4523 individual claims for personal injury and damages were submitted to the Canary Islands Government's Single Register of Affected People, it should be noted that these claims may also include cases of damage or loss outside the analysed perimeter of the lava (due to tephra fall, gas contamination). In terms of economic losses, the total amount according to the ECB would be 1147 million euros, of which 98% would be capital stock losses associated with damage to goods, infrastructure and property, mostly agricultural (90%), residential (7%), industrial (~1%) and road (~1%). The Ministry of Taxes, Budgets and European Affairs (Canary Islands Government) estimated total post-disaster losses to public and private assets at 842 million euros (Mixed Commission for the Reconstruction Recovery and Support of La Palma, 2022), which was later raised to 982 million euros (COMUNICAN, 19/04/2022), approaching the ECB-based damage estimate of more than one billion euros. If the compensation attributable to the central State are included, the amount would be even closer to the ECB-based estimate, since compensations paid out by the Insurance Compensation Consortium (Spanish Government) exceeded 220 million euros according to data provided by the organisation. In any

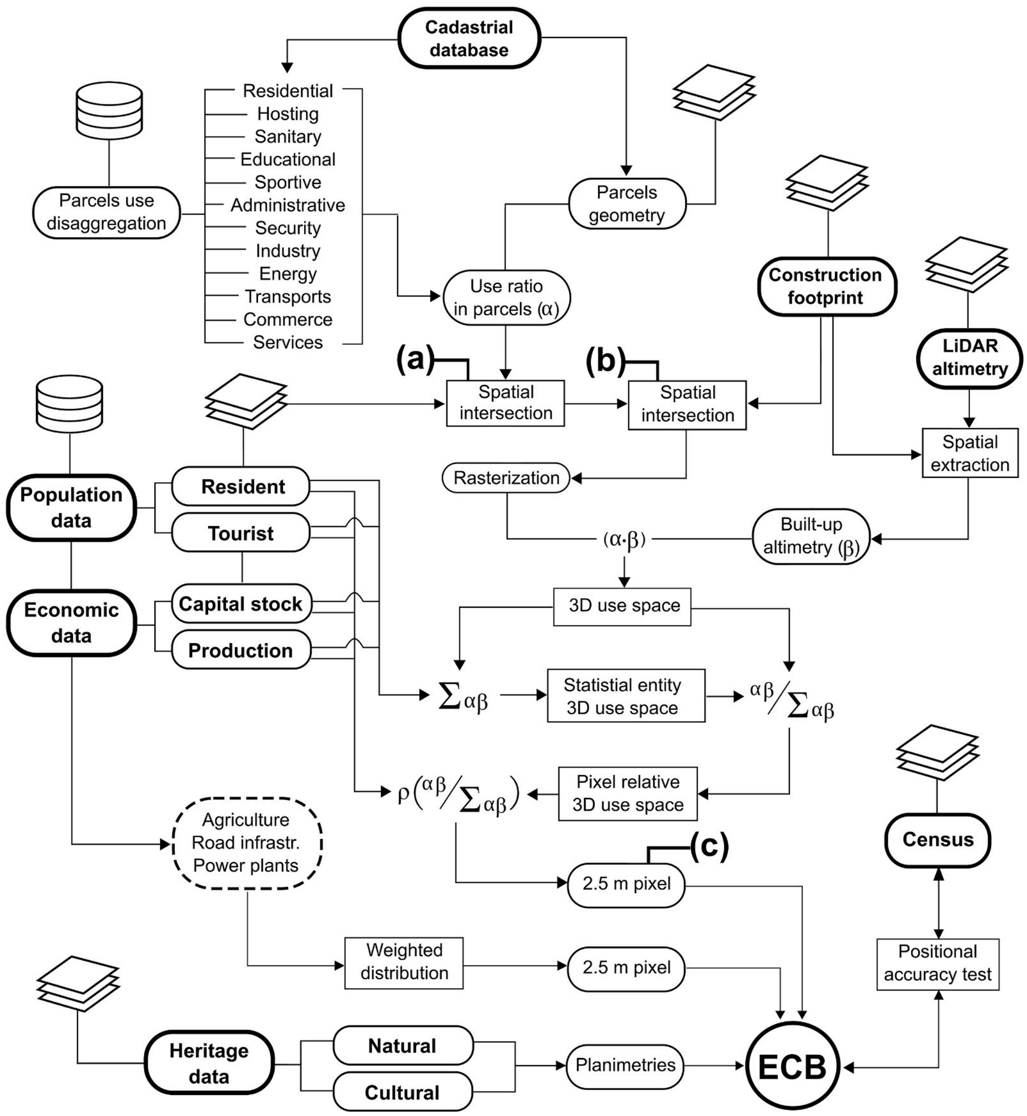

Fig. 4. General graphical downscaling procedure using the example of the capital stock of residential infrastructure at municipal level.

case, the ECB-based economic valuation is very close to the post-disaster valuations. The value shown in the ECB fits the actual damage value due to the accuracy of the ECB with the real scale and the full vulnerability to lava flows (no resistance capacity) of the exposed infrastructures.

4.3. Exposure and damages in the 2019 major wildfire of Gran Canaria

In August 2019, in conditions of high temperatures, low atmospheric humidity and strong winds, four wildfires affected 6.1% of the surface area of Gran Canaria. The two most impacted regions were Artenara and Valleseco, with 1137.60 and 8498.80 hm^2 affected, respectively (Copernicus EMS, 2019). The event was the largest wildfire of 2019 in Spain (Europa Press, 22/01/2020). The largest outbreak originated near the town of Valleseco, at an altitude of over 1000 m, and spread westwards (Fig. 6).

The affected area was predominantly forest and agricultural with a low population density. The evacuation affected about 10,000 people in 56 population centres (EFE, 23/08/2019; Zamarreño-Aramendia et al., 2020). Based on the low-resolution global human settlement (GHS) population grid, the Copernicus rapid mapping service (Copernicus EMS, 2019) estimated that more than 13,000 people were affected within the fire's perimeter, but according to the high-resolution ECB the resident population in the affected area was approximately 3000 people.

The ECB-based estimate of assets exposure was over 750 million euros, 90% of which were cadastral values of agricultural estates whose capital stock was not affected during the wildfire. The main economic losses were due to production downtime and damages to residential and road infrastructure. The ECB estimates an exposed value of 28 million euros for residential infrastructure, 38 million euros for road infrastructure and more than 12 million euros for annual productivity across the different productive sectors (Table 3). Private insurers indemnified the Gran Canaria Island Council with 7.3 million euros for damage to publicly owned property (MAPFRE Corporate News, 12/06/2020). In turn, Gran Canaria Island Council paid out more than 5 million euros for damage to real estate and production losses (Gran Canaria Island Council, 2019) and the Spanish Government approved almost 6 million euros for disaster-induced damage (Royal Decree-Law 11/2019, Spanish Government). The compensation values amounted to around 18 million euros, which corresponds to approximately 23% of the ECB's exposed damage value. This reflects the different fire intensities (Copernicus EMS, 2019), as well as the different degrees of resistance of exposed elements.

However, the most important impacts of the Artenara and Valleseco wildfire were on ecosystems and natural heritage. The fire penetrated 5 areas of the Canary Islands Network of Natural Protected Areas (NPA), 5 protected areas of the Natura 2000 network and 7 geosites catalogued by

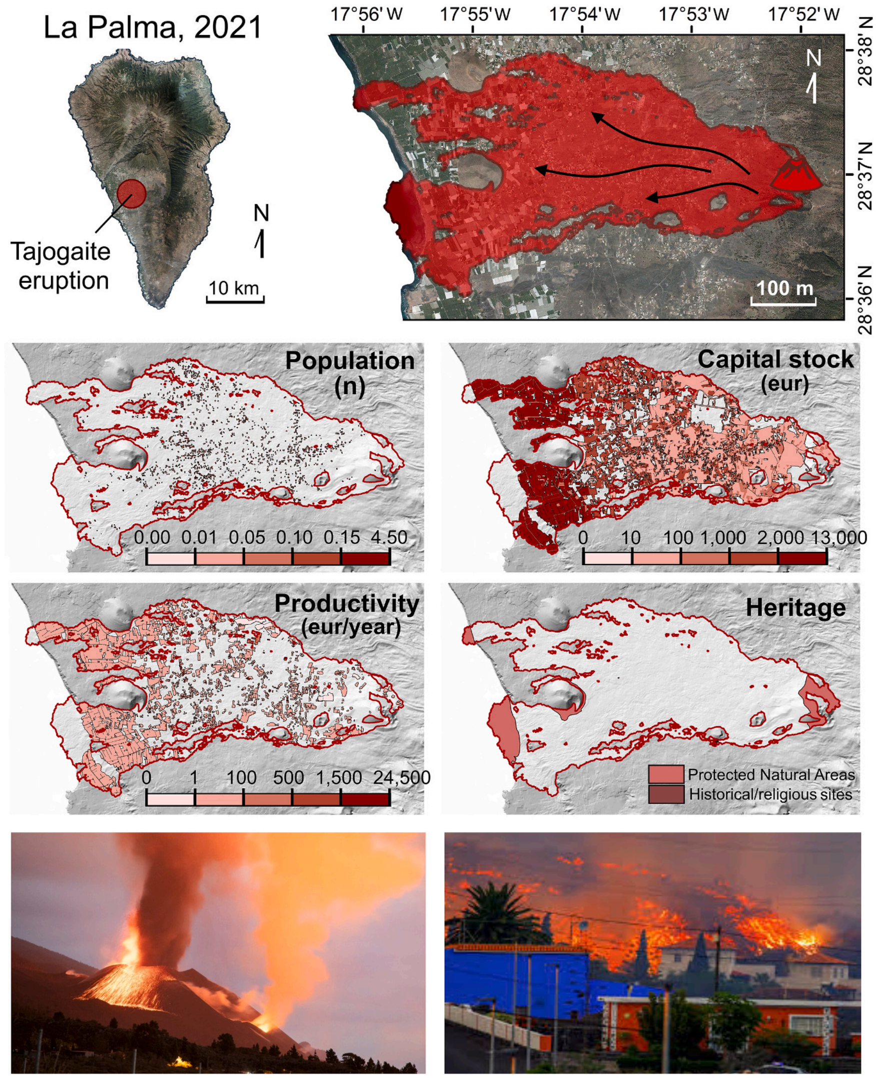

Fig. 5. Exposure of population, capital stock, productivity and heritage in the area of the 2021 Tajogaite volcano eruption on La Palma (Canary Islands). The values correspond to 6.25 m^2 cells. At the bottom, press photos of the 2021 Tajogaite volcano eruption.

the Geological and Mining Institute of Spain, affecting a total of 9834.6 hm^2 (Table 3). The biggest impact was on the Tamadaba pine forest, classified as a Natural Park of the NPA network and a Special Bird Conservation Area of the Natura 2000 network.

4.4. Exposure and damages in the 2018 coastal flooding of Garachico

The town of Garachico, on the north coast of Tenerife, is one of the most historically critical points in the Canary Islands archipelago in terms of coastal flooding (Yanes, 2012, pp. 355–358). The local underwater topography, marked by great depths at a short distance from the coast and bathymetric irregularities, means that the storms affecting the north of the island acquire greater severity at this point. In the last 25 years, approximately every 2 years there has been a damaging coastal flooding event in this locality according to data provided by the Insurance Compensation Consortium (Spanish Government).

One of the largest events recorded in recent decades occurred on the night of 17-18 November 2018. The waves overtopped the coastal protections and penetrated the locality, leading to the evacuation of 39 people (Diario de Avisos, 19/11/2018) of the 116 (mostly tourists in this case) that were exposed in the area of the flooding according to the ECB (Table 3). Economic assets of around 12 million euros were exposed to the flood according to the ECB (Table 3), of which approximately half was capital stock, real estate and infrastructure, while the other half corresponded to annual productive capital flow from the tertiary sector. According to data provided by the Insurance Compensation Consortium (Government of Spain), this agency awarded 807,000 euros in post-event compensation, mainly for damage to housing, shops and hotel facilities. Once again, the actual damages were significantly lower than the assets exposed due to the different intensity of the event (depth of flooding and flow velocity) and the resilience of the assets. Apart from the risks to persons and economic damages, potential damage to historical heritage is of particular concern in Garachico, which is home to up to 8 cultural heritage sites, three of which were exposed to the 2018 flood event, although no severe damage was reported for any of them.

5. Discussion

5.1. Methodological constraints to the sources availability

This work used the most accurate data available in the Canary Islands (Table 1) to generate a hazard exposure map based on the downscaling of aggregate indicators. Deployment of the method was possible thanks to the very complete geographical information available in the Canary Islands (Figs. 2 and 4). The Canary Islands are politically and administratively part of the European Union, so there are more

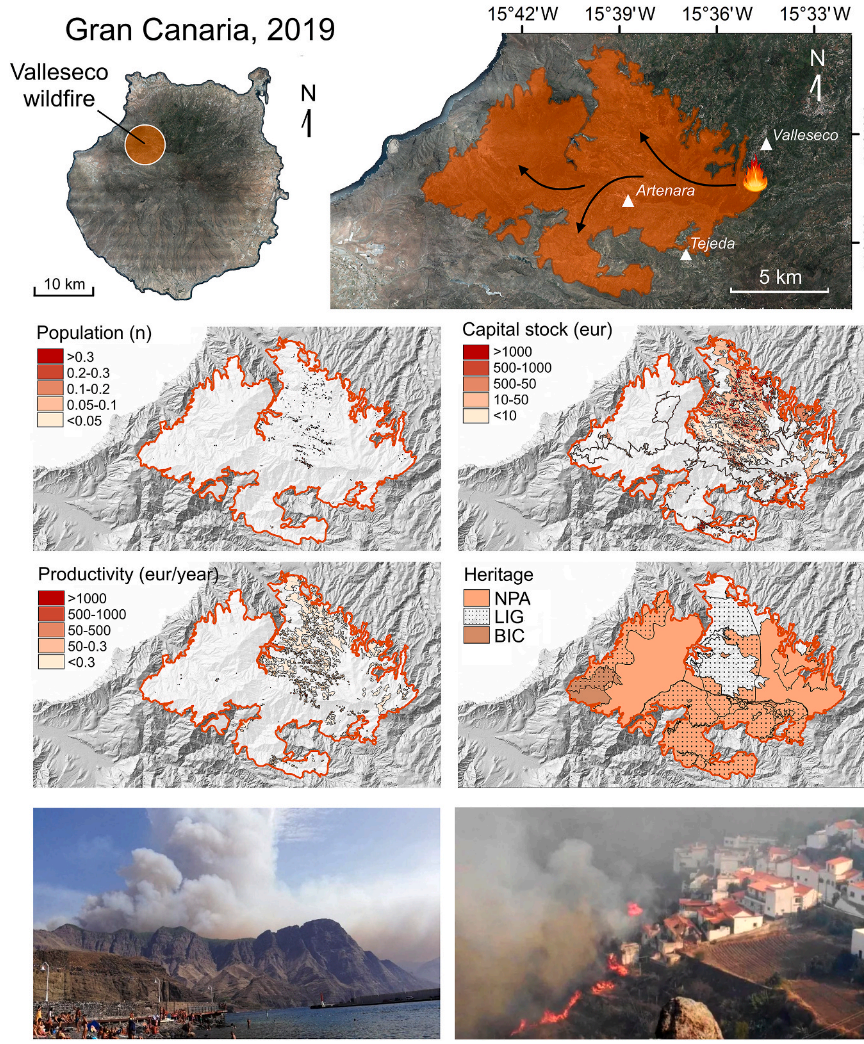

Fig. 6. Exposure of population, capital stock, productivity and heritage in the area of the 2019 Artenara and Valleseco wildfire on the island of Gran Canaria. The correspond to 6.25 m^2 cells. The perimeter of the fire was obtained from the Copernicus rapid mapping service (European Commission, 2015). NPA = Natural Protected Area; LIG = Sites of Geological Interest (Spanish initials); BIC = Assets of Cultural Interest (Spanish initials). At the bottom, press photos of the 2019 Artenara and Valleseco wildfire.

datasets available compared to most other volcanic island countries in the world (e.g., complete cadastral censuses, LiDAR altimetry surveys). A lack of spatial data in other territories would require adjustments. In the absence of complete cadastral censuses, land use maps could be used, as has been tested in multiple works (e.g., Chen et al., 2004; Eicher and Brewer, 2001; Mennis, 2009), and the lack of detailed planimetries and altimetries could be overcome by remote sensing techniques based on aerial and satellite image processing (e.g., Ehrlich et al., 2018). However, remotely sensed land use maps cannot reach the thematic accuracy of censuses, especially in urban areas, and so the accuracy of the results will largely depend on the scale of the input sources. Spain's Land Occupation Data System (SIOSE for its initials in Spanish) generates maps at a scale of 1:25,000 with uses proportionally presented, which would allow an identical application of the method although with less accurate results. Likewise, the use of population census sections (INE, Government of Spain), with an average surface area of ~58 hm^2 in the Canary Islands, are valid but will yield less accurate results.

New computer algorithms, GIS software and remote sensing acquisition systems have facilitated the possibility of processing large volumes of information and producing extensive digital cartographic databases using these resources. The method developed in this work has the virtue of combining the cadastral approach (Maantay et al., 2007; Mora-García and Marti-Ciriquian, 2015; Preciado; 2015) with the volumetric approach (Keiler et al., 2006; Lwin and Murayama, 2011) in a novel way. The sequence of dasymetric operations allowed downscaling statistical entities to cadastral parcels, built-up footprints and finally pixel volumetry. It has been found that such an approach is not only valid for population downscaling but also has the potential for the construction of complete exposure mapping bases including economic indicators. Regarding the population distribution, the procedure could present limitations in the consideration of the size of dwellings and the existence of empty dwellings and second homes (Mora-García and Marti-Ciriquian, 2015). We verified that the built-up volume has at least 84% of explanatory power on the population distribution in the Canary Islands (Fig. 3), but the remaining 16% could be related to these factors not considered in the model.

5.2. Additional risk factors and ECB accuracy

The ECB shows a high correspondence with the actual scale (Tables 2 and 3) and can therefore constitute a solid basis for forecasting impacts of natural events in a multi-hazard territory such as the Canary Islands. However, as risk is also composed of hazard and vulnerability factors (e.g., Bruen and Dzakpasu, 2018; Chen et al., 2004; Fuchs et al., 2012; IPCC, 2014; Lirer et al., 2010; Schneiderbauer and Ehrlich, 2004), further progress needs to be made to complete a comprehensive risk base

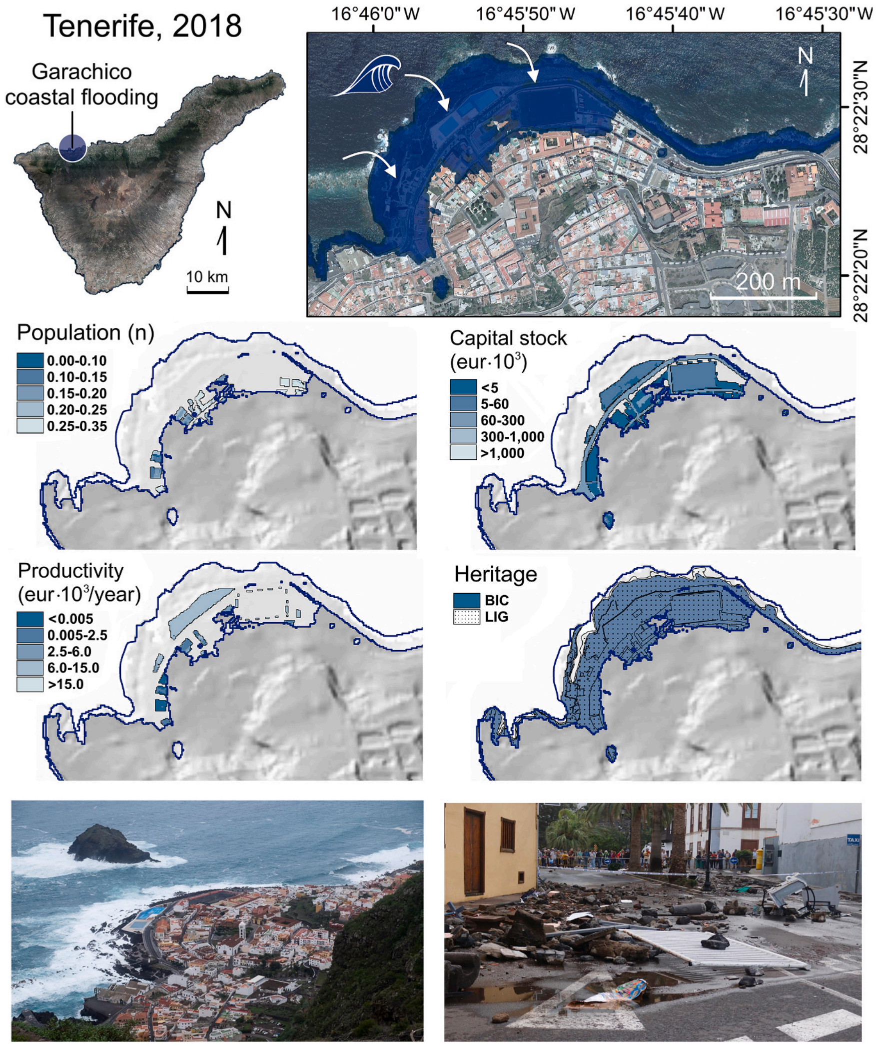

Fig. 7. Exposure of population, capital stock, productivity and heritage, in the 2018 coastal flood area of Garachico on the island of Tenerife. The values correspond to 6.25 m^2 cells. The flood area corresponds to the simulation of a 50-year wave return period (SITCAN, Canary Islands Government). BIC = Assets of Cultural Interest (Spanish initials); LIG = Sites of Geographical Interest (Spanish initials). At the bottom, press photos of the 2018 coastal flood event of Garachico.

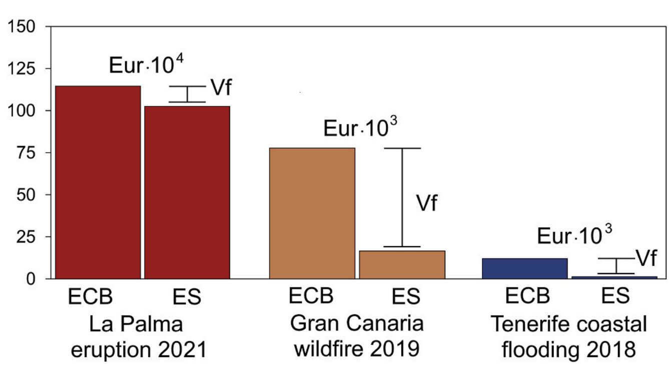

Fig. 8. Comparison between the ECB exposure of economic value and actual damage estimates from external sources (ES) in the 2021 eruption of La Palma, 2019 wildfire of Gran Canaria and 2018 flooding of Tenerife. The differences between the two values are due to the vulnerability factor (Vf).

that allows accurate damage forecasts. The non-inclusion of a vulnerability variable is the main factor of uncertainty in the BCE-based impacts analysis. Exposure captures only the set of people, property and assets at risk, but not their damageability. Due to the resistance and recovery factor of the physical elements, and the different spatial intensities of the hazardous phenomenon, damage will always be equal to or less than the exposed total. The exposed value is equal to the total value, and so the damage is equal to the exposed value only in case of full damage, as in the case of the Tajogaite eruption (Fig. 8). This means that a complete risk assessment should include vulnerability to avoid overestimations. Including vulnerability in the ECB is necessary to reduce the uncertainty associated with forecasting actual impacts. It is a highly complex factor because each element presents a different vulnerability to each type and degree of hazard. In the Tajogaite eruption, the value of the actual damage almost coincided with the value of the exposed assets because the force of the event exceeded the resistance of any structure (Table 3, Figs. 5 and 8). However, in the coastal flooding of Garachico and the wildfire of Artenara and Valleseco, the value of the actual damage was below the value of the exposed assets due to the resistance of the structures (Table 3, Figs. 6, Figs. 7 and 8). Magnitude-damage curves, for example, are functions that assign a degree of damage to each degree of process magnitude, being physical approximations of vulnerability (e.g., Huizinga et al., 2017).

The ECB would also benefit from the inclusion of eco-system services associated with natural heritage, including their economic translation. The limitation of the ECB in assessing the socio-economic impacts of ecosystem destruction can be seen, for example, in the Artenara and Valleseco wildfires of 2021 (Gran Canaria), where the greatest impact was ecological. Incorporation of the indirect economic impact of the conservation or destruction of elements of the natural environment would provide a more realistic and complete approximation of the total impact of both natural and anthropogenic disasters.

Climate change will bring increased risks to island territories, making spatial tools for forecasting and damage assessment more necessary than ever. The impending intensification of risk will be due to the combined effect of increased hazards and an increase in exposed assets and their vulnerability. In this regard, the ECB, combined with vulnerability estimations, has already been used to estimate the effects of sea level rise in the Canary Islands through the PIMA ADAPTA Costas project (Canary Islands Government, 2022). According to projections made with the ECB, vulnerability parameters and physical models, in 2100 up to 2% of the population and 11% of the GDP of the Canary Islands will be at risk due to the effects of coastal flooding in the worst case climate scenarios analysed in the project.

6. Conclusions

Oceanic islands are small and fragmented territories, often remote and subject to multiple natural hazards. Inherent hazards include geological (seismicity, volcanism, slope dynamics) and meteorological processes (cyclones, river and coastal flooding, droughts, fires). A proper understanding of these risks implies a detailed knowledge of the exposure factor (i.e., the distribution of the people and assets exposed to potential damage). However, this data is often insufficient or aggregated in statistical entities that do not adequately serve the needs of disaster prevention and management.

As a representative example, the Canary Islands are a densely populated multi-risk territory where most of the socio-economic data are aggregated in municipal or supra-municipal entities and whose scale does not allow an adequate comparison with high-resolution physical hazard models. Therefore, this work developed a downscaling methodology based on hybrid dasymetric procedures (cadastral and volumetric) to establish an exposure cartographic base (ECB) in the Canary Islands that allows more accurate risk assessments. The availability of complete cadastral censuses, large-scale planimetries and high-resolution altimetric models has made it possible to estimate the distribution of multiple infra- and supra-municipal socio-economic indicators at a scale of 2.5 m and construction units. In territories with less geographic information available, the method presented will have to be adapted to the sources, which may affect its precision and accuracy.

The cross-checking of the ECB with different survey censuses enabled determination of an optimum level of thematic-positional accuracy in the results. Furthermore, its testing with three recent real events revealed the importance of the vulnerability factor in damage estimation and the need to develop it on the basis of the ECB. The actual damage estimate for the Tajogaite eruption was very close to the ECB's estimate of exposed people and assets, as vulnerability to lava flows is close to a constant level of 100%. However, the actual damages in the 2019 Gran Canaria wildfire and the 2018 Tenerife coastal flooding were significantly lower than the exposed elements in the ECB because of the different spatial intensity of the hazard and the different vulnerabilities of the exposed elements. It should also be noted that the ECB could be enriched by the evaluation of ecosystem services and indirect economic impacts of the destruction of the natural environment. Nevertheless, the proposed procedure has made it possible to establish a solid cartographic basis for the detailed assessment of natural hazards in an archipelagic region such as the Canary Islands, which could be replicated in other territories where socio-economic information is excessively aggregated for risk assessment purposes.

Funding sources

The work was developed in the framework of the PIMA ADAPTA COSTAS Canarias project, financed by the Ministry for Ecological Transition and the Demographic Challenge of the Spanish Government and coordinated by the Regional Ministry of Ecological Transition, Fight against Climate Change and Territorial Planning of the Government of the Canary Islands. First author Nicolás Ferrer is beneficiary of the Postdoctoral programme Catalina Ruiz 2021 of the Canary Islands Government and the European Social Fund.

CRediT authorship contribution statement

Nicolás Ferrer: Writing – review & editing, Writing – original draft, Methodology, Investigation, Formal analysis, Data curation, Conceptualization. **Gustavo Herrera:** Writing – review & editing, Resources, Funding acquisition, Conceptualization.

References

Allgeyer, S., Quentel, É., Hébert, H., Gailler, A., & Loevenbruck, A. (2017). Tsunami hazard in La Réunion Island (SW Indian Ocean): Scenario-based numerical modelling on vulnerable coastal sites. *Pure and Applied Geophysics, 174*(8), 3123–3145.

Andrew, N. L., Bright, P., de la Rua, L., Teoh, S. J., & Vickers, M. (2019). Coastal proximity of populations in 22 pacific island countries and territories. *PLoS One, 14*(9), Article e0223249.

Arango, T., Healy, J., & Cave, D. (2023). *Maui knew dangerous wildfires had become inevitable*. NA-NA: It Still Wasn't Ready. International New York Times.

Audru, J. C., Bitri, A., Desprats, J. F., Dominique, P., Eucher, G., Hachim, S., … Terrier-Sedan, M. (2010). Major natural hazards in a tropical volcanic island: A review for Mayotte island, Comoros archipelago, Indian ocean. *Engineering Geology, 114*(3–4), 364–381.

Bachèlery, P., Morin, J., Villeneuve, N., Soulé, H., Nassor, H., & Ali, A. R. (2015). Structure and eruptive history of Karthala volcano. In *Active volcanoes of the southwest Indian ocean: Piton de La fournaise and Karthala* (pp. 345–366). Berlin, Heidelberg: Springer Berlin Heidelberg.

Bruen, M., & Dzakpasu, M. (2018). *WARNDIS project final report: A review of climate change-related hazards and natural disaster vulnerabilities and of agencies involved in warning and disaster management*. Ireland: Environmental Protection Agency.

Burby, R. J. (Ed.). (1998). *Cooperating with nature: Confronting natural hazards with land-use planning for sustainable communities*. Joseph Henry Press.

Callaghan, J. (2019). A short note on the intensification and extreme rainfall associated with Hurricane Lane. *Tropical Cyclone Research and Review, 8*(2), 103–107.

Campbell, J. R. (2019). *Urbanisation and natural disasters in Pacific Island countries*. Policy Brief No: Toda Peace Institute.

Carracedo, J. C., Troll, V. R., Day, J. M., Geiger, H., Aulinas, M., Soler, V., & Albert, H. (2022). The 2021 eruption of the Cumbre Vieja volcanic ridge on La Palma, canary islands. *Geology Today, 38*(3), 94–107.

Carvalho, E. C. (1980). Engineering aspects of the january 1st, 1980 Azores earthquake. *Proceedings of the 7th World Conference on Earthquake Engineering, Istanbul, 9*, 477–489.

Chen, K., McAneney, J., Blong, R., Leigh, R., Hunter, L., & Magill, C. (2004). Defining area at risk and its effect in catastrophe loss estimation: A dasymetric mapping approach. *Applied Geography, 24*(2), 97–117.

Civico, R., Ricci, T., Scarlato, P., Taddeucci, J., Andronico, D., Del Bello, E., … Pérez, N. M. (2022). High-resolution digital surface model of the 2021 eruption deposit of Cumbre Vieja volcano, La Palma, Spain. *Scientific Data, 9*(1), 435.

Couto, F. T., Salgado, R., & Guiomar, N. (2021). Forest fires in Madeira Island and the fire weather created by orographic effects. *Atmosphere, 12*(7), 827.

Ehrlich, D., Melchiorri, M., Florczyk, A. J., Pesaresi, M., Kemper, T., Corbane, C., & Siragusa, A. (2018). Remote sensing derived built-up area and population density to quantify global exposure to five natural hazards over time. *Remote Sensing, 10*(9), 1378.

Eicher, C. L., & Brewer, C. A. (2001). Dasymetric mapping and areal interpolation: Implementation and evaluation. *Cartography and Geographic Information Science, 28*(2), 125–138.

European Commission, Joint Research Centre (JRC). (2015). *GHS-POP R2015A - GHS population grid, derived from GPW4, multitemporal (1975, 1990, 2000, 2015) - OBSOLETE RELEASE*. European Commission, Joint Research Centre (JRC). http://data.europa.eu/89h/jrc-ghsl-ghs_pop_gpw4_globe_r2015a.

FEMA. (2002). *Technical manual of HAZUS®99: Earthquake loss estimation methodology*. Washington, DC: Federal Emergency Management Agency. Available from: http://www.fema.gov/HAZUS/.

Ferrer, N., Marrero-Rodríguez, N., Sanromualdo-Collado, A., Vegas, J., & García-Romero, L. (2023). Early morphodynamics of the sudden formation of beaches during the 2021 volcanic eruption of La Palma. *Geomorphology, 436*, 108779.

Formetta, G., & Feyen, L. (2019). Empirical evidence of declining global vulnerability to climate-related hazards. *Global Environmental Change, 57*, 101920.

Fragoso, M., Trigo, R. M., Pinto, J. G., Lopes, S., Lopes, A., Ulbrich, S., & Magro, C. (2012). The 20 february 2010 Madeira flash-floods: Synoptic analysis and extreme rainfall assessment. *Natural Hazards and Earth System Sciences, 12*(3), 715–730.

Fuchs, S., Birkmann, J., & Glade, T. (2012). Vulnerability assessment in natural hazard and risk analysis: Current approaches and future challenges. *Nat Hazards, 64*, 1969–1975.

Fuchs, S., Röthlisberger, V., Thaler, T., Zischg, A., & Keiler, M. (2017). Natural hazard management from a coevolutionary perspective: Exposure and policy response in the European Alps. *Annals of the Association of American Geographers, 107*(2), 382–392.
Gallego, F. J., Batista, F., Rocha, C., & Mubareka, S. (2011). Disaggregating population density of the European Union with CORINE land cover. *International Journal of Geographical Information Science, 25*(12), 2051–2069.
García-Rodríguez. (2023). *Informe-dictamen sobre los efectos demográficos, sociales y económicos de la erupción volcánica de la palma de 2021 realizado a propuesta de Gesplan*. Gobierno de Canarias. chrome-extension. efaidnbmnnnibpcajpcglclefindmkaj/https://minioapi.devops.grafcan.es/prclp/230714-Dictamen-volcan-JLG-version-7_12deJuliode2023.pdf.
Geiger, T. (2018). Continuous national gross domestic product (GDP) time series for 195 countries: Past observations (1850-2005) harmonized with future projections according to the shared socio-economic pathways (2006-2100). *Earth System Science Data, 10*(2), 847–856.
Genzano, N., Marchese, F., Plank, S., & Pergola, N. (2023). Monitoring the mauna loa (Hawaii) eruption of november–december 2022 from space: Results from GOES-R, sentinel-2 and landsat-8/9 observations. *International Journal of Applied Earth Observation and Geoinformation, 122*, Article 103388.
Hernandez-Pacheco, A., & Valls, M. C. (1982). The historic eruptions of La Palma island (Canaries). *Arquipelago: Serie Ciencias da Natureza, 3*, 83–94.
Holt, J. B., & Lu, H. (2011). Dasymetric mapping for population and sociodemographic data redistribution. *Urban remote sensing: Monitoring, synthesis and modeling in the urban environment, 250*, 195–210.
Huizinga, J., de Moel, H., & Szewczyk, W. (2017). *Global flood depth-damage functions. Methodology and the database with guidelines*.
HVRI. (2015). *Spatial hazard events and losses database for the United States, version 14.1. [Online database] columbia, SC: Hazards and vulnerability research Institute*. University of South Carolina.
Iglesias, V., Braswell, A. E., Rossi, M. W., Joseph, M. B., McShane, C., Cattau, M., & Travis, W. R. (2021). Risky development: Increasing exposure to natural hazards in the United States. *Earth's Future, 9*(7), Article e2020EF001795.
Jega, I. M. (2015). *Estimating population surfaces in areas where actual distributions are unknown: Dasymetric mapping and pycnophylactic interpolation across different spatial scales*. Doctoral dissertation, University of Leicester.
Jongman, B., Winsemius, H. C., Aerts, J. C., Coughlan de Perez, E., Van Aalst, M. K., Kron, W., & Ward, P. J. (2015). Declining vulnerability to river floods and the global benefits of adaptation. *Proceedings of the National Academy of Sciences, 112*(18), E2271–E2280.
Keiler, M. (2004). Development of the damage potential resulting from avalanche risk in the period 1950-2000, case study Galtür. *Natural Hazards and Earth System Sciences, 4*(2), 249–256.
Keiler, M., Sailer, R., Jörg, P., Weber, C., Fuchs, S., Zischg, A., & Sauermoser, S. (2006). Avalanche risk assessment-a multi-temporal approach, results from Galtür, Austria. *Natural Hazards and Earth System Sciences, 6*(4), 637–651.
Kummu, M., Taka, M., & Guillaume, J. H. (2018). Gridded global datasets for gross domestic product and Human Development Index over 1990-2015. *Scientific Data, 5*(1), 1–15.
Lerner-Lam, A. (2007). Assessing global exposure to natural hazards: Progress and future trends. *Environmental Hazards, 7*(1), 10–19.
Lirer, L., Petrosino, P., & Alberico, I. (2010). Hazard and risk assessment in a complex multi-source volcanic area: The example of the campania region, Italy. *Bulletin of Volcanology, 72*, 411–429.
López-Saavedra, M., & Martí, J. (2023). Reviewing the multi-hazard concept. Application to volcanic islands. *Earth-Science Reviews, 236*, Article 104286.
Lwin, K. K., & Murayama, Y. (2011). Estimation of building population from LIDAR derived digital volume model. In *Spatial analysis and modeling in geographical transformation process: GIS-based applications* (pp. 87–98).
Maantay, J. A., Maroko, A. R., & Herrmann, C. (2007). Mapping population distribution in the urban environment: The cadastral-based expert dasymetric system (CEDS). *Cartography and Geographic Information Science, 34*(2), 77–102.
Masson, D. G., Le Bas, T. P., Grevemeyer, I., & Weinrebe, W. (2008). Flank collapse and large-scale landsliding in the Cape Verde islands, off west Africa. *Geochemistry, Geophysics, Geosystems, 9*(7).
Meldau, A. (2013). Cyclone evan in Samoa. *The state of environmental migration, 1*, 49–62.
Mennis, J. (2003). Generating surface models of population using dasymetric mapping. *The Professional Geographer, 55*(1), 31–42.
Mennis, J. (2009). Dasymetric mapping for estimating population in small areas. *Geography Compass, 3*(2), 727–745.
Mixed Commission for the Reconstruction, Recovery and Support of La Palma. (2022). *Informe sobre las actuaciones y medidas emprendidas tras la erupción del volcán de Cumbre Vieja (La Palma), seis meses después del inicio de la emergencia*. Madrid: Agencia Estatal Boletín Oficial del Estado.
Mora-García, R. T., & Marti-Ciriquian, P. (2015). Desagregación poblacional a partir de datos catastrales. In J. de la Riva, et al. (Eds.), *Análisis espacial y representación geográfica: Innovación y aplicación*. Zaragoza: Universidad de Zaragoza; AGE, 2015.
Okal, E. A., Fritz, H. M., Synolakis, C. E., Borrero, J. C., Weiss, R., Lynett, P. J., … Chan, I. C. (2010). Field survey of the Samoa tsunami of 29 September 2009. *Seismological Research Letters, 81*(4), 577–591.
INE. (2022). *Población por comunidades, edad (año a año), Españoles/Extranjeros, Sexo y Año*. https://www.ine.es/jaxi/Datos.htm?path=/t20/e245/p08/l0/&file=02003.px#!tabs-mapa.
IPCC. (2014). In R. K. Pachauri, & L. A. Meyer (Eds.), *Climate change 2014: Synthesis report. Contribution of working groups I, II and III to the fifth assessment report of the intergovernmental panel on climate change [core writing team* (p. 151). Geneva, Switzerland: IPCC.
Paprotny, D., Sebastian, A., Morales-Nápoles, O., & Jonkman, S. N. (2018). Trends in flood losses in Europe over the past 150 years. *Nature Communications, 9*(1), 1985.
Pelling, M., & Uitto, J. I. (2001). Small island developing states: Natural disaster vulnerability and global change. *Global Environmental Change Part B: Environmental Hazards, 3*(2), 49–62.
Pesaresi, M., Ehrlich, D., Kemper, T., Siragusa, A., Florczyk, A., Freire, S., & Corban, C. (2017). *Atlas of the human planet 2017: Global exposure to natural hazards*. Luxembourg: EUR 28556 EN, Publications Office of the European Union, 2017.
Petak, W. J., & Atkisson, A. A. (1982). *Natural hazard risk assessment and public policy: Anticipating the unexpected (No. 04; GB5014, P4*. New York: Springer-Verlag.
Preciado, J. M. S. (2015). La cartografía catastral y su utilización en la desagregación de la población. Aplicación al análisis de la distribución espacial de la población en el municipio de Leganés (Madrid). *Estudios Geográficos, 76*(278), 309–333.
Ramalho, R. S., Winckler, G., Madeira, J., Helffrich, G. R., Hipólito, A., Quartau, R., & Schaefer, J. M. (2015). Hazard potential of volcanic flank collapses raised by new megatsunami evidence. *Science Advances, 1*(9), Article e1500456.
Richmond, B. M., Fletcher, C. H., III, Grossman, E. E., & Gibbs, A. E. (2001). Islands at risk: Coastal hazard assessment and mapping in the Hawaiian islands. *Environmental Geosciences, 8*(1), 21–37.
Schneiderbauer, S., & Ehrlich, D. (2004). Risk, hazard and people's vulnerability to natural hazards. A review of definitions, concepts and data. *European Commission Joint Research Centre. EUR, 21410*, 40.
Su, M. D., Lin, M. C., Hsieh, H. I., Tsai, B. W., & Lin, C. H. (2010). Multi-layer multi-class dasymetric mapping to estimate population distribution. *Science of the Total Environment, 408*(20), 4807–4816.
Thomas, B. E. O., Roger, J., Gunnell, Y., & Ashraf, S. (2023). A method for evaluating population and infrastructure exposed to natural hazards: Tests and results for two recent Tonga tsunamis. *Geoenvironmental disasters, 10*(1), 4.
Tobin, G. A. (1997). *Natural hazards: Explanation and integration*. New York: Guilford Press.
Tobler, W. R. (1979). Smooth pycnophylactic interpolation for geographical regions. *Journal of the American Statistical Association, 74*(367), 519–530.
Troll, V. R., Junca, M. A., Carracedo, J. C., Geiger, H., Torrado, F. J. P., Soler, V., … Dayton, K. K. (2023). The 2021 La Palma eruption; social dilemmas resulting from living close to an active volcano. *EarthArXiv, Preprint*. https://doi.org/10.31223/X5QX1M
Vargas, R. (2023). In *Estudio territorial para abordar los trabajos de recuperación del Valle de Aridane tras la crisis eruptiva. Gobierno de Canarias. chrome-extension.* efaidnbmnnnibpcajpcglclefindmkaj/https://minioapi.devops.grafcan.es/prclp/230628_LPM_atlas_230523.pdf.
Ward, S. N., & Day, S. (2001). Cumbre Vieja volcano—potential collapse and tsunami at La Palma, canary islands. *Geophysical Research Letters, 28*(17), 3397–3400.
Williams, S., Paulik, R., Weaving, R., Bosserelle, C., Chan Ting, J., Wall, K., … Scheele, F. (2021). Multiscale quantification of tsunami hazard exposure in a pacific small island developing state: The case of Samoa. *GeoHazards, 2*(2), 63–79.
Wright, T. L., Chun, J. Y. F., Esposo, J., Heliker, C., Hodge, J., Lockwood, J. P., & Vogt, S. M. (1992). Map showing lava-flow hazard zones. *Island of Hawaii: U.S. Geological Survey Miscellaneous Field Studies Map MF-2193, scale, 1*, 250, 000.
Wu, S. S., Qiu, X., & Wang, L. (2005). Population estimation methods in GIS and remote sensing: A review. *GIScience and Remote Sensing, 42*(1), 80–96.
Yanes, A. (2012). *Temporales marinos y ocupación costera en Garachico (NO de Tenerife)*. Santander: XII Reunión Nacional de Geomorfología.
Yanes, A. (2017). Desastres naturales en Canarias. La costa como espacio de riesgo en Tenerife. *Semina: Ciências Sociais e Humanas*, (29).
Zamarreño-Aramendia, G., Cristòfol, F. J., de-San-Eugenio-Vela, J., & Ginesta, X. (2020). Social-media analysis for disaster prevention: Forest fire in Artenara and Valleseco, canary islands. *Journal of Open Innovation: Technology, Market, and Complexity, 6*(4), 169.

Resources

COMUNICAN (19/04/. (2022). *Los daños por la erupción en La Palma alcanzan los 982 millones de euros*. Portal de noticias del Gobierno de Canarias https://www3.gobiernodecanarias.org/noticias/los-danos-por-la-erupcion-en-la-palma-alcanzan-los-982-millones-de-euros/.
Copernicus Emergency Management Service. (2019). *Valleseco: Delineation product, monitoring 2*. version 2, release 1 https://emergency.copernicus.eu/mapping/list-of-components/EMSR382.
Decree-Law 1/2022 of 20 January, por el que se adoptan medidas urgentes en materia urbanística y económica para la construcción o reconstrucción de viviendas habituales afectadas por la erupción volcánica en la isla de La Palma. BOE» núm. 76, de 30 de marzo de 2022, páginas 41833 a 41842 https://www.boe.es/eli/es-cn/dl/2022/01/20/1.
DGSE. (2014). *Plan Especial de Protección Civil y Atención de Emergencias por Incendios Forestales de la Comunidad Autónoma de Canarias (INFOCA). Gobierno de Canarias*. https://www.gobiernodecanarias.org/boc/2014/113/007.html.
D. de Avisos (19/11/2018) '39 evacuados en Garachico por el oleaje que llegó a una tercera planta' https://diariodeavisos.elespanol.com/2018/11/la-borrasca-deja-en-canarias-mas-de-40-litros-por-metro-cuadrado-y-vientos-de-mas-de-100-kmh/.
EFE (23/08/2019) 'Espacio y especies de gran valor ecológico afectados en incendio Gran Canaria'. https://efeverde.com/espacio-especies-gran-valor-ecologico-afectados-incendio-gran-canaria/.
Europa Press. (2019). *(22/01/2020). 'El incendio de Gran Canaria, con más de 10.000 hectáreas quemadas, el peor de España en*. https://www.europapress.es/islas-canarias/

noticia-incendio-gran-canaria-mas-10000-hectareas-quemadas-peor-espana-2019-20200122180208.html.

ISTAC. (2018). *Malla estadística eurostat adaptada a Canarias*. Instituto Canario de Estadística, Gobierno de Canarias. https://datos.canarias.es/catalogos/estadisticas/dataset/malla-estadistica-eurostat-adaptada-a-canarias-celdas-250-m-de-lado.

MAPFRE Corporate News (12/06/2020) 'La indemnización de MAPFRE al Cabildo de Gran Canaria por los daños del incendio del verano de 2019 alcanzó los 7,3 m €'. https://www.mapfre.com/comunicacion/negocio-espana-comunicacion/mapfre-cabildo-gran-canaria-indemnizacion-73millones/#:~:text=Una%20vez%20concluidas%20las%20complejas,aseguradas%2C%20titularidad%20del%20Cabildo%20de.

Proyecto PIMA Adapta Costas Canarias. (2021). *SITCAN, Portal de datos abiertos del Gobierno de Canarias*. https://opendata.sitcan.es/dataset/pima-adapta-costas-canarias.

Royal Decree-Law 11/2019 of 20 September 2019, por el que se adoptan medidas urgentes para paliar los daños causados por temporales y otras situaciones catastróficas. «BOE» núm. 227, de 21 de septiembre de 2019, páginas 103903 a 103916 (14 págs.) https://www.boe.es/buscar/doc.php?id=BOE-A-2019-13409.